The mRNACalc web server accounts for the hypochromicity of modified nucleosides and enables the accurate quantification of nucleoside-modified mRNA.

Authors: Esteban Finol*[1], Sarah E. Krul[2], Sean J. Hoehn[2], Carlos E. Crespo-Hernández*[2].

These authors contributed equally: Sarah E. Krul and Sean J. Hoehn.

* To whom correspondence should be addressed.

[1] Programme in Emerging Infectious Diseases, Duke-NUS Medical School, National University of Singapore, Singapore, 169857, Singapore.

[2]Department of Chemistry, Case Western Reserve University, Cleveland, Ohio, 44106, United States of America.

E-mail address: esteban.finol@duke-nus.edu.sg ; carlos.crespo@case.edu

Graphical Abstract:

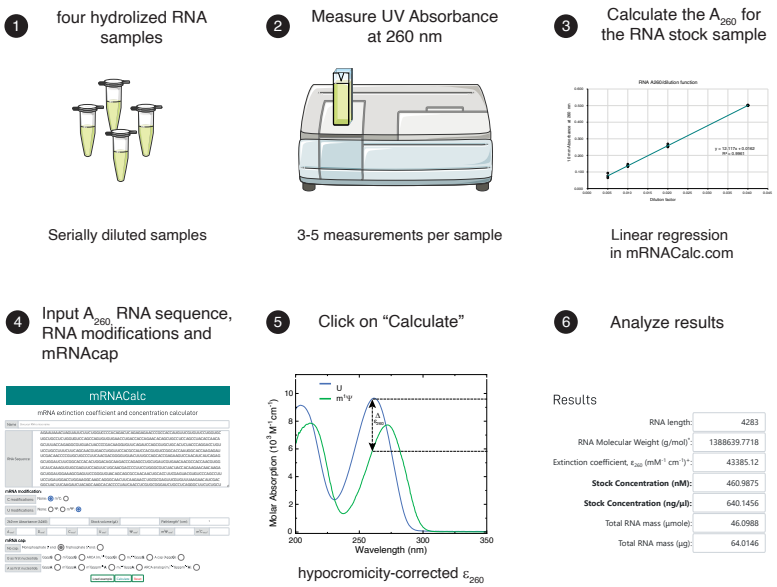

Abstract:

Nucleoside-modified mRNA technologies necessarily incorporate N^1-methylpseudouridine into the mRNA molecules to prevent over-stimulation of cytoplasmic RNA sensors. Despite this modification, mRNA concentrations remain mostly determined through measurement of UV absorbance at 260 nm wavelength (A_{260}). Herein, we report that the N^1-methylpseudouridine absorbs approximately 40% less UV light at 260 nm than uridine, and its incorporation into mRNAs leads to the under-estimation of nucleoside-modified mRNA concentrations, with 5-15% error, in a mRNA sequence dependent manner. We therefore examined the RNA quantification methods and developed the mRNACalc web server. It accounts for the molar absorption coefficient of modified nucleotides at 260 nm wavelength, the RNA composition of the mRNA and the A_{260} of the mRNA sample to enable accurate quantification of nucleoside-modified mRNAs. The webserver is freely available at https:\\www.mrnacalc.com.

38 **Introduction:**

39 The therapeutic use of messenger RNA (mRNA) has sparked great optimism in the
40 development of novel vaccines and therapeutics against a myriad of infectious or yet
41 incurable diseases (1). The mRNA technology enables the production of antigenic,
42 functional, and/or therapeutic proteins by introducing mRNA into the human body and
43 cells (2). Since mRNAs act in the cytoplasm transiently, they do not bear any risk of
44 integration into the host cell genome. Most importantly, the mRNA technology enables
45 rapid, cost-efficient and scalable production, which is free of cellular (cell cultures) or
46 animal materials (3). Thus, mRNA technologies facilitate manufacturing and allow for
47 a rapid response to emerging infectious diseases, as emphatically underscored by the
48 rapid rollout of COVID-19 mRNA vaccines in many parts of the world. Modified
49 nucleosides, such as pseudouridine (Ψ), N^1-methylpseudouridine ($m^1\Psi$) and 5-
50 methylcytidine (m^5C), are often incorporated into the mRNA molecules; such
51 modifications reduce stimulation of cytoplasmic RNA sensors, such as toll-like
52 receptor 3 and 7, for improved safety profiles and enhance mRNA translation (4, 5).
53 However, how modified nucleosides affect mRNA concentration measurements and
54 potentially confound pre-clinical dosing, efficacy, and toxicology studies, which could
55 make or break further clinical development of any therapeutic, remains undefined.

56 The determination of RNA concentration often relies on measurements of its UV
57 absorbance at 260 nm wavelength (A_{260}) and the implementation of the Beer–Lambert
58 law (6). The accuracy of these measurements is scattered by the variable
59 hypochromicity of RNA due to its sequence-dependent folding. The molar absorption
60 coefficient (MAC or extinction coefficient, ε) of a folded RNA at 260 nm (ε_{260}) is reduced
61 as compared to its unfolded state (7). This difference is buffer- and concentration-
62 dependent and arises from changes in the chemical environment of the nucleobases
63 – the main chromophore, due to base-pairing, stacking, intermolecular interactions,
64 and other conformational changes. Considering these variabilities, a rough estimation
65 for the ε_{260} of any single stranded RNA (40 µg/ml per absorbance unit) is extensively
66 used and its associated ±10–20 % error in the estimation of RNA concentration is
67 widely accepted (6). This error range may suffice to assess dose-response for mRNA
68 therapeutics across several orders of magnitude *in celula* or *in vivo* experiments. Yet
69 it would be valuable to know concentrations at higher accuracy for the development of
70 mRNA technologies. Our particular concern is in measurements of self-amplifying

RNAs (saRNA) and nucleoside-modified mRNAs. The logarithmic amplification of saRNA can convert a 20 % accepted error in RNA concentration into a several fold differences in dose-response between one experiment and the subsequent replicates. The chemical modifications on the nucleobases of mRNA can also induce profound changes in the mRNA MAC, hindering the accurate quantification of nucleoside-modified mRNA concentrations.

To attain greater accuracy in RNA quantification, RNA molecules are hydrolysed prior UV absorbance determination using a combination of thermal and alkaline hydrolysis (6, 8). The RNA hydrolysis shifts the hypochromic folded state of the RNA to the hyperchromic state of the single monophosphate nucleotides (9). Since the precise MAC of the four standard nucleotides in aqueous buffered solution are known, the molar absorption of any hydrolysed mRNA can be calculated as the sum of the molar absorption of its nucleotide compositions. Thus, upon the determination of the 260 nm UV absorbance (A_{260}), the RNA concentration can be quantified with an error of ~ 4 % using these methods (6). However, the incorporation of modified nucleosides can alter the RNA molar absorption and increase the error of the measurements in an RNA sequence-dependent manner.

Herein, we report our effort to revisit and determine the molar absorption coefficients of modified nucleosides (Ψ, $m^1\Psi$ and m^5C). We also examined three different methods for RNA hydrolysis and provided them along with the mRNACalc web server. This web tool incorporates the most recently revised ε_{260} for standard, modified and mRNA capping nucleosides, allowing the accurate determination of standard and nucleoside-modified mRNAs using UV spectroscopy. Once the RNA sequence, the A_{260} and the RNA stock volume values are provided as input, the mRNACalc web server calculates the RNA stock concentration in nM and ng/µl and the total RNA mass in µmole and µg.

97 **Results and discussion:**

98 To assess the impact of chemical modifications on the spectrophotometric parameters
99 of nucleosides for mRNA quantification, we examined the modified nucleosides that
100 have recently been employed in nucleoside-modified mRNA technologies:
101 pseudouridine (Ψ), N^1-methyl-pseudouridine ($m^1\Psi$), and 5-methylcytidine (m^5C).
102 Pseudouridine is an isomer of uridine – the standard nucleoside in RNA.
103 Pseudouridine, as opposed to other nucleosides, is a carbon-carbon ribofuranosyl
104 nucleoside, i.e., the uracil nucleobase is linked to the ribose through its fifth carbon,
105 instead of a N^1-linkage (10). This unique arrangement places the N^1-imino group
106 toward the so-called "C-H" edge of the pyrimidine ring and confers additional
107 properties to this edge in pseudouridine. This imino hydrogen proton is susceptible to
108 hydrogen bonding, chemical exchange, and chemical modifications such as N^1-
109 methylation. Thus, the N^1-methyl-pseudouridine, as well as the m^5C, represents a
110 modification of the C-H edge of the pyrimidine nucleobase. A similar 5-methyl
111 modification also differentiates uridine from thymidine. The influence of a 5-methyl
112 substituent on the UV absorbance of pyrimidine rings is well known since the 1940's
113 when Sister Miriam Michael Stimson showed that it provokes a subtle reduction in
114 molar absorbance and a shift of the peak maximum (λ_{max}) to a longer wavelength
115 (lower energy) – the so-called bathochromic or red shift (11–14). For uridine to
116 thymidine and cytidine to 5-methylcytidine, the respective peak shifts ($\Delta\lambda_{max}$) are + 5
117 and + 7 nm with a 3 % and 1.3 % reduction in the UV molar absorption ($\Delta\varepsilon_{max}$) at λ_{max}
118 (Fig.1a). For the Ψ to $m^1\Psi$, we have observed a similar bathochromic shift ($\Delta\lambda_{max}$ = +
119 7 nm and $\Delta\varepsilon_{max}$ = - 1.7 %, Fig. 1b). More importantly, $m^1\Psi$ is hypochromic as compared
120 to uridine at λ_{max} ($\Delta\varepsilon_{max}$ = - 21 %) and, due to the bathochromic shift, $m^1\Psi$ absorbs
121 39.8 % less UV than uridine at 260 nm (Fig. 1c). Thus, the substitution of uridine by
122 $m^1\Psi$ in mRNA technologies can lead to substantial changes in the spectrophotometric
123 properties of the mRNA and may lead to the underestimation of nucleoside-modified
124 mRNA concentrations.

125 To assess whether the complete U-to-$m^1\Psi$ substitution alter the UV absorbance of an
126 mRNA, three mRNAs were transcribed using either U, Ψ, or $m^1\Psi$. These mRNA also
127 encoded a double-Broccoli aptamer in their 3' untranslated region. Once the DFHBI-
128 1T fluorophore was bound to the G-quadruplex in the Broccoli aptamer, the mRNA

129 emitted green light upon excitation (15). By normalizing the UV absorbance (A_{260}) of

Fig. 1: The nucleobase methylation and its bathochromic effect on the UV molar absorption spectra of pyrimidines and nucleoside-modified mRNAs.

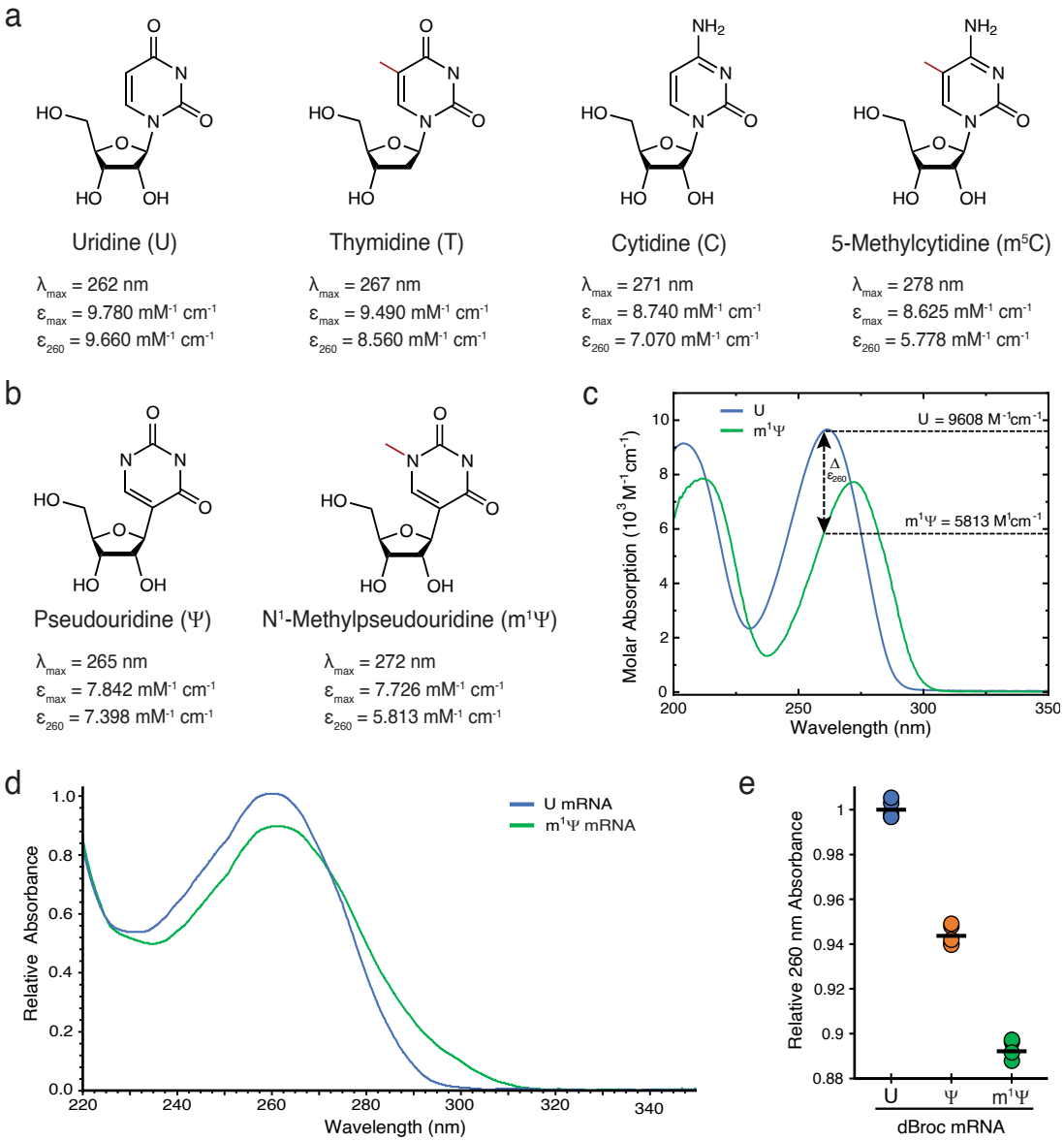

a, Skeletal formula of uridine, thymidine, cytidine and 5-methylcytidine. The methyl substituents are highlighted in red. Thymidine, a 2'-deoxy nucleoside, is the natural form of 5-methyluridine. The λ_{max}, ε_{max} and ε_{260} values are provided. References are provided in the supplementary section. **b**, Skeletal formula of pseudouridine and N1-methylpseudouridine. The methyl substituents are highlighted in red. The λ_{max}, ε_{max} and ε_{260} values are also provided. **c**, Steady-state absorption spectra of uridine (light blue line) and N1-methylpseudouridine (green line) at pH 7.4. The ε_{260} for U and $m^1\Psi$ are shown. **d**, Relative UV absorption curves from mRNAs with uridine or N1-methylpseudouridine nucleosides. They were normalized to the corresponding F507 values and plotted relative to the peak maximum (ε_{max}) of the U mRNA. **e**, The relative A_{260}/F_{507} values from five replicates of the U-, Ψ-, and $m^1\Psi$-mRNAs are shown, the black line corresponds to the average absorbance. Values are relative to the average absorbance of the U-mRNA. The three comparisons of the mean relative A_{260}/F_{507} values were significant (t-test; $p < 0.005$).

130 each mRNA by its corresponding fluorescence (F_{507}), it was observed that in practice
131 the relative UV absorbance of the nucleoside-modified mRNA was significantly
132 reduced as compared to the standard mRNA (ΔA_{260} = -10.6%, Fig. 1d and 1e).
133 Importantly, the UV absorption spectrum of the $m^1\Psi$ mRNA depicted a broad
134 absorption peak and a red shift, which brings additional implications for the
135 assessment of the RNA sample purity (Supplementary section). These findings
136 indicate that, for accurate determination of nucleoside-modified mRNA concentrations
137 and proper interpretation of dose-ranging preclinical studies, the UV spectroscopic
138 changes must be accounted for to prevent under-estimating mRNA concentrations by
139 5 to 15%, depending on the proportion of $m^1\Psi$ in the mRNA composition.

140 To enable accurate measurement of nucleoside-modified mRNA, we assessed
141 different RNA hydrolysis and built an experimental workflow for the determination of
142 mRNA concentrations. The modern analytical use of alkaline hydrolysis of RNA is
143 known since 1922, when Steudel and Peiser demonstrated that 1 M NaOH hydrolysed
144 yeast RNA, whereas thymus DNA resisted the NaOH hydrolysis (16). The alkali-
145 promoted transesterification of RNA occurs due to the nucleophilic attack of the 2'-OH
146 in the ribose to the 3',5'-phosphodiester bond, explaining the alkali-resistance of the
147 2'-deoxyribonucleotides (Fig. 2a) (17). This reaction is further catalysed with the
148 introduction of heat. However, the combination of thermal and alkaline hydrolysis, e.g.,
149 1 M NaOH at 95°C, also catalyses the deamination of cytosine to uridine in a small
150 percentage of residues (18, 19). Thus, a compromise between the two methods is
151 often applied. In our hands, three of such protocols showed a similar change in A_{260}
152 upon hydrolysis of yeast RNA – a historical standard sample for these methods. (Fig.
153 2b). These protocols are provided in the mRNACalc web server along with the
154 implementation of a linear regression model from multiple measurements at serial
155 dilutions to reduce the impact of sample handling variation (Fig. 2c).

156 Taken together, by incorporating modified nucleoside MAC parameters, accounting
157 for the actual mRNA nucleotide composition, and providing an experimental workflow,
158 the mRNACalc web server represents a freely available and all-inclusive tool for the
159 determination of nucleoside-modified mRNA concentrations using UV spectroscopy.

Fig. 2: The mRNACalc webserver and the photometric measurement of RNA concentrations rely on the intrinsic UV molar absorption properties of nucleotides.

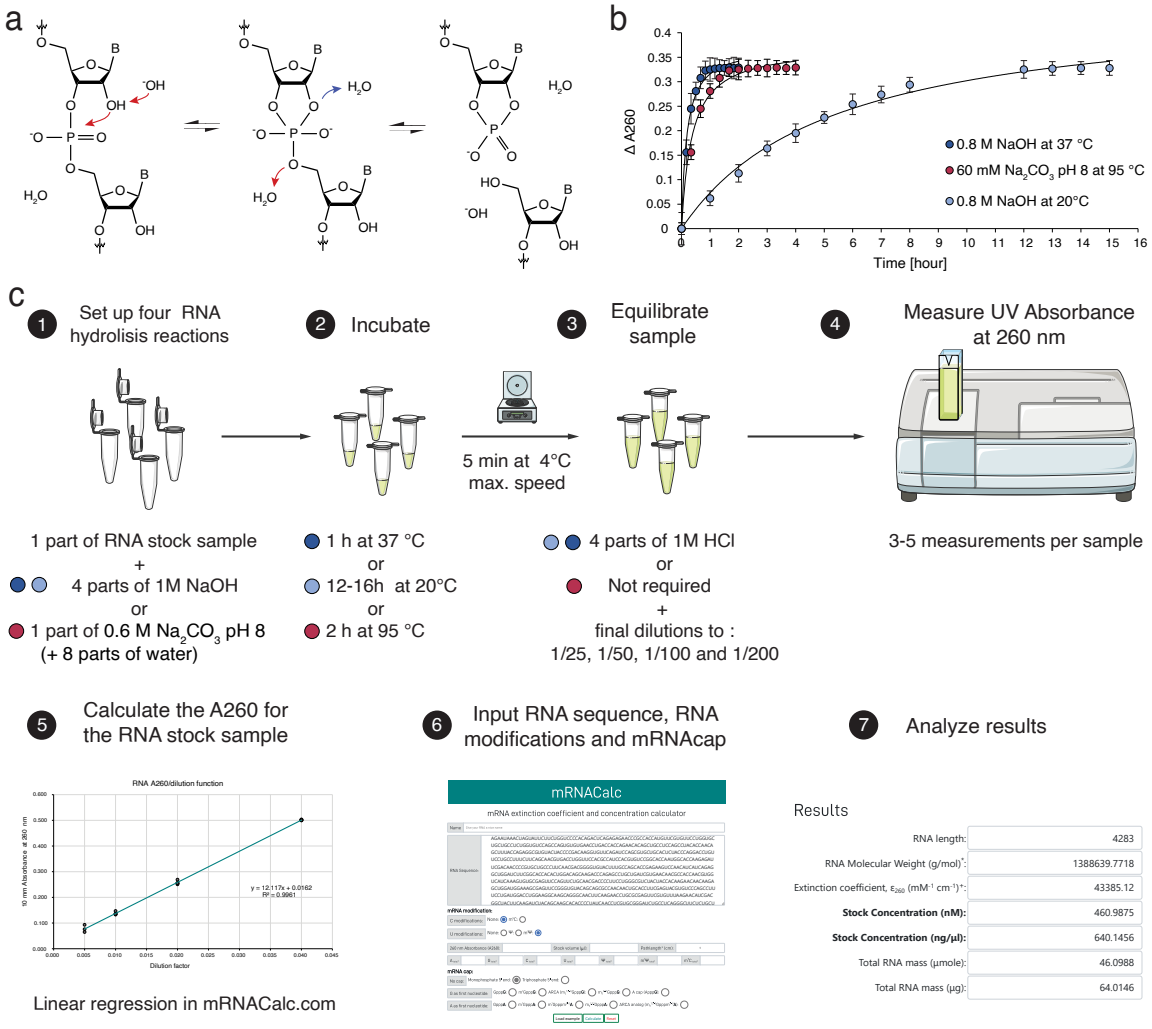

a, Alkali-promoted transesterification allows RNA hydrolysis and mRNA quantification. Under alkaline conditions, the reactive -OH triggers the nucleophilic attack of the 2'-OH on the 3',5'-phosphodiester linkage, converting the ground-state configuration of RNA into a penta-coordinated intermediate and leading to a 2'3'-cyclic phosphodiester. This cyclic form is then known to form 3' and 2' monophosphate nucleotides (not shown). **b**, Thermal and/or alkaline hydrolysis of RNA over time. Yeast RNA was hydrolysed using three different previously described methods and the ΔA_{260} was determined using an UV spectrophotometer at different intervals. For expedite RNA hydrolysis (1- or 2-hours incubation), a combination of thermal and alkaline hydrolysis can be used (dark blue dots, 0.8 M NaOH at 37°C; red dots, 0.5 M Na_2CO_3 pH 8 at 95°C). For overnight incubation, alkaline hydrolysis suffices (light blue dots, 0.8 M NaOH at 20°C, the last four measurements were performed after an overnight incubation). Dots indicate the mean value of three measurements. Error bars correspond to standard deviations. **c**, Experimental workflow for the determination of RNA concentration using the mRNACalc web server. The coloured dots refer to the different RNA hydrolysis methods in 2.b.

162 **Materials and Methods:**

163 The Beer-Lambert experiments.

164 N1-methylpseudouridine ($m^1\Psi$, >95% purity) and Uridine (Urd, 99% purity) were
165 purchased from Biosynth Carbosynth and Sigma-Aldrich, respectively, and were used
166 as received. Phosphate buffer solutions with a total phosphate concentration of 16 mM
167 from monosodium and disodium phosphate salts dissociated in ultrapure water (Milli-
168 pore) were freshly prepared on the day of each experiment. The pH of the solution
169 was adjusted using 0.1 M solutions of NaOH and HCl to the desired pH of 7.4 (± 0.1
170 pH units). Steady-state absorption was recorded using a Cary 100 spectrometer.
171 Serial dilutions of known concentration were carried out such that the absorbance
172 reading at the respective lambda maximum (local maximum absorbance) remained
173 below 1.0, within the linear range of the instrument. The molar absorption coefficients
174 were experimentally determined using the slope from the linear regression from
175 plotting absorbance versus concentration. The correlation constant for the linear
176 regression analysis of the Beer-Lambert's Law data for determining molar absorption
177 constants was >0.9999 showing a strong linear relationship.

178 mRNA *in vitro* transcription and purification.

179 The Plasmid DNA template (pUCIDT plasmid) was grown in DH5 alpha *E. coli* (New
180 England Biolabs Inc.) in 300 ml of Luria-Bertani broth supplemented with Kanamycin
181 (50 µg/ml) and a maxi preparation was performed using the QIAGEN® Plasmid Plus
182 Maxi Kit following manufacturer instructions. The plasmid encoded a T7 promoter
183 followed by the mCherry gene with a degradation tag (1449 nucleotides) plus the 3'
184 and 5' untranslated regions (UTR) of the BNT162b2 mRNA vaccine (541 nucleotides).
185 The double broccoli aptamer was encoded within the poli-adenine region in the 3'UTR.
186 The plasmid was linearized by EcoRV restriction enzyme digestion at the end of the 3'
187 UTR.

188 A standard T7 transcription reaction included 30 mM Tris-HCl, pH 7.9, 2 mM
189 spermidine, 30 mM $MgCl_2$, 5 mM NaCl, 10 mM DTT, 50 µg/ml BSA (New England
190 Biolabs Inc.), 0.005% Triton X-100, 2% polyethylene glycol (PEG8000), 5 mM of each
191 triphosphate ribonucleotide (standard nucleotides were purchased from Jena
192 Bioscience GmBH and pseudouridine and N1-methylpseudouridine from BOC
193 sciences), 2 µM linearized plasmid DNA template, 3.5 µM T7 RNA Polymerase (in

194 house produced and purified) and 0.0025 units of *E. coli* inorganic PPase (New
195 England Biolabs, Inc). All reagents were purchased from Sigma-Aldrich, unless
196 otherwise stated. The reactions were incubated at 37 °C for 2.5 hours and stopped by
197 the addition of 500 mM EDTA, pH 8 to a final concentration of 35 mM.

198 The mRNA was purified using anion exchange chromatography. A PRP-X600 Anion
199 exchange column (Hamilton Company, Inc.) was equilibrated in Buffer A (85:15 100
200 mM TRIS, pH 8/Acetonitrile). RNA samples were loaded onto the column at a flow rate
201 of 3 ml/min and eluted with a 40-minutes gradient of 0-40% buffer B (85:15 100 mM
202 TRIS 2.5 M LiCl, pH 8/Acetonitrile). Fractions containing the mRNA were collected and
203 the mRNA molecules were precipitated using standard Butanol extraction (20). The
204 purity of the mRNA preparation was assessed using high-resolution automated
205 electrophoresis in the Agilent 2100 Bioanalyzer system using the Bioanalyzer RNA
206 6000 pico assay (Agilent Technologies, Inc).

207 Determination of the mRNA UV absorption spectrum.

208 To determine the UV absorption spectrum of mRNAs, the mRNAs stocks were diluted
209 to approximately 25 nM into a buffer containing 40 mM HEPES pH 7.4, 5 mM $MgCl_2$,
210 and 100 mM KCl to a final volume of 2 ml. Five independent mRNA samples were
211 prepared per mRNA set (U-, Ψ-, and $m^1\Psi$-mRNA). The UV absorption spectra were
212 recorded for each mRNA sample using in a UV-3600i plus UV-VIS spectrophotometer
213 (Shimadzu Corp.).

214 Excitation-emission experiments on the DFHBI-1T bound mRNAs.

215 After UV absorption determination, the mRNA samples were bound to the DFHBI-1T
216 fluorophore, by adding 100 µM DFHBI-1T, 100% DMSO to a 500 nM concentration
217 into the 2-ml mRNA samples. Fluorescence was measured using a Fluorolog-3
218 spectrofluorometer (Horiba Scientific) using the excitation and emission wavelengths
219 commonly used for DFHBI-1T (Excitation: 472 nm, emission: 507 nm) (15).

220 Determination of the relative UV absorbance (A_{260}).

221 The A_{260}/F_{507} ratios were calculated for each mRNA sample. The mean A_{260}/F_{507}
222 values for U-, Ψ-, and $m^1\Psi$-mRNA were calculated. The A_{260}/F_{507} values of each
223 sample were normalized using the mean A_{260}/F_{507} value from the U-mRNA as
224 reference and they were plotted in a dot plot. The t-tests were applied to compare the

225 mean A_{260}/F_{507} values across each pair of mRNA sets, using a p-values of 0.005 as
226 cut-off of significance.

227 Methods of RNA hydrolysis:

228 Two methods of RNA hydrolysis were tested in this study. Torula yeast RNA was used
229 as standard RNA sample (Sigma-Aldrich). The Yeast RNA stock was prepared at 1000
230 µg/µl in water. Thus, after 1/25 dilution, the UV absorbance of this RNA sample would
231 be within the linear range of the instrument (UV-3600i plus UV-VIS spectrophotometer,
232 Shimadzu Corp.).

233 The most extensively used alkaline RNA hydrolysis method involves adding 1 part of
234 RNA and 4 parts of 1 M NaOH and incubating them at 37°C for 1 hour (21). To test
235 this method, twelve yeast RNA samples were hydrolysed. Every 10 minutes, a sample
236 was neutralised with 4 parts of 1 M HCl and diluted to 1/25 with 16 parts of water.
237 Three UV absorbance measurements were performed on every sample. Similarly, a
238 room temperature variation of this method is often used for overnight RNA hydrolysis.
239 Therefore, twelve RNA samples were hydrolysed and incubated at 20°C for up to 15
240 hours. Samples were neutralized and diluted hourly followed by three UV absorbance
241 measurements.

242 A second method of thermal hydrolysis at neutral pH was also tested (8). To test this
243 method, twelve yeast RNA samples hydrolysed (1 part of RNA in 9 parts of 60 mM
244 Na_2CO_3 pH 8) with an incubation of at 95°C for up to 2 hours. Every 20 minutes, a
245 sample was diluted to 1/25 with 15 parts of water and three UV absorption
246 measurements were performed on every sample.

247 **References**

248 1. Chaudhary, N., Weissman, D. and Whitehead, K.A. (2021) mRNA vaccines for
249 infectious diseases: principles, delivery and clinical translation. *Nat Rev Drug*
250 *Discov*, **20**, 817–838.

251 2. Sahin, U., Karikó, K. and Türeci, Ö. (2014) mRNA-based therapeutics —
252 developing a new class of drugs. *Nat Rev Drug Discov*, **13**, 759–780.

253 3. Webb, C., Ip, S., Bathula, N.V., Popova, P., Soriano, S.K.V., Ly, H.H., Eryilmaz,
254 B., Nguyen Huu, V.A., Broadhead, R., Rabel, M., *et al.* (2022) Current Status
255 and Future Perspectives on MRNA Drug Manufacturing. *Mol Pharm*,
256 10.1021/acs.molpharmaceut.2c00010.

257 4. Karikó, K., Muramatsu, H., Welsh, F.A., Ludwig, J., Kato, H., Akira, S. and
258 Weissman, D. (2008) Incorporation of Pseudouridine Into mRNA Yields
259 Superior Nonimmunogenic Vector With Increased Translational Capacity and
260 Biological Stability. *Molecular Therapy*, **16**, 1833–1840.

261 5. Andries, O., Mc Cafferty, S., De Smedt, S.C., Weiss, R., Sanders, N.N. and
262 Kitada, T. (2015) N1-methylpseudouridine-incorporated mRNA outperforms
263 pseudouridine-incorporated mRNA by providing enhanced protein expression
264 and reduced immunogenicity in mammalian cell lines and mice. *Journal of*
265 *Controlled Release*, **217**, 337–344.

266 6. Cavaluzzi, M.J. and Borer, P.N. (2004) Revised UV extinction coefficients for
267 nucleoside-5′-monophosphates and unpaired DNA and RNA. *Nucleic Acids*
268 *Res*, **32**, e13.

269 7. Tinoco, I. Jr. (1960) Hypochromism in Polynucleotides. *J. Am. Chem. Soc.*, **82**,
270 4785–4790.

271 8. Wilson, S.C., Cohen, D.T., Wang, X.C. and Hammond, M.C. (2014) A neutral pH
272 thermal hydrolysis method for quantification of structured RNAs. *RNA*, **20**,
273 1153–1160.

274 9. Doty, P., Boedtker, H., Fresco, J.R., Haselkorn, R. and Litt, M. (1959) Secondary
275 structure in ribonucleic acids. *Proceedings of the National Academy of*
276 *Sciences*, **45**, 482–499.

277 10. Cohn, W.E. (1960) Pseudouridine, a Carbon-Carbon Linked Ribonucleoside in
278 Ribonucleic Acids: Isolation, Structure, and Chemical Characteristics. *Journal*
279 *of Biological Chemistry*, **235**, 1488–1498.

280 11. Stimson, M.M. (1949) The Ultraviolet Absorption Spectra of Some Pyrimidines.
281 Chemical Structure and the Effect of pH on the Position of λmax. *J. Am.*
282 *Chem. Soc.*, **71**, 1470–1474.

283 12. Sharonov, A., Gustavsson, T., Marguet, S. and Markovitsi, D. (2003)
284 Photophysical properties of 5-methylcytidine. *Photochem Photobiol Sci*, **2**,
285 362–364.

13. Shugar, D. and Fox, J.J. (1952) Spectrophotometric studies of nucleic acid derivatives and related compounds as a function of pH: I. Pyrimidines. *Biochimica et Biophysica Acta*, **9**, 199–218.

14. Rabczenko, A. and Shugar, D. (1971) Studies on the conformation of nucleosides, dinucleoside monophosphates and homopolynucleotides containing uracil or thymine base residues, and ribose, deoxyribose or 2'-O-methylribose. *Acta Biochim Pol*, **18**, 387–402.

15. Filonov, G.S., Moon, J.D., Svensen, N. and Jaffrey, S.R. (2014) Broccoli: Rapid Selection of an RNA Mimic of Green Fluorescent Protein by Fluorescence-Based Selection and Directed Evolution. *J. Am. Chem. Soc.*, **136**, 16299–16308.

16. Steudel, H. and Peiser, E. (1922) Über Nucleinsäure-Eiweißverbindungen. **122**, 298–306.

17. Lipkin, D., Talbert, P.T. and Cohn, M. (1954) The Mechanism of the Alkaline Hydrolysis of Ribonucleic Acids. *J. Am. Chem. Soc.*, **76**, 2871–2872.

18. Wang, R.Y.-H., Kuo, K.C., Gehrke, C.W., Huang, L.-H. and Ehrlich, M. (1982) Heat- and alkali-induced deamination of 5-methylcytosine and cytosine residues in DNA. *Biochimica et Biophysica Acta (BBA) - Gene Structure and Expression*, **697**, 371–377.

19. Shen, J.C., Rideout, W.M. and Jones, P.A. (1994) The rate of hydrolytic deamination of 5-methylcytosine in double-stranded DNA. *Nucleic Acids Res*, **22**, 972–976.

20. Green, M.R. and Sambrook, J. (2017) Concentrating Nucleic Acids by Extraction with Butanol. *Cold Spring Harb Protoc*, **2017**, pdb.prot093401.

21. Bock, R.M. (1967) Alkaline hydrolysis of RNA. In *Methods in Enzymology*, Nucleic Acids, Part A. Academic Press, Vol. 12, pp. 224–228.

Code availability

The webserver is available at https:\\www.mrnacalc.com. The website is free and open to all users and there is no login requirement.

The source code for mRNACalc webserver is available under GNU general public licence from https://github.com/estebanfbfc/mRNACalc.

Contributions

E.F. conceived the study. E.F. and C.E.C-H. supervised the project. E.F. developed the mRNACalc webserver. S.E.K. and S.J.H. performed the Beer-Lambert experiments and prepared the corresponding figure panel. E.F. performed the relative absorbance of mRNA experiments and analysed the data. E.F. prepared figures, wrote the initial draft of the manuscript and edited the submitted version of the manuscript with contributions from all the authors.

Acknowledgement

The authors would also like to thank Prof. Eng Eong Ooi for his invaluable advice and generosity throughout this work and Prof. Guillermo C. Bazan for providing access to the UV-Vis and fluorescence spectrometers in his laboratory.

Funding

This work was supported by the National Medical Research Council through an Open Fund - Large Collaborative Grant, granted to Prof. Eng Eong Ooi, and by the National Science Foundation (Grant No. CHE-2246805), granted to Prof. Carlos E. Crespo-Hernández.

Conflict of interest statement. Authors declare no competing interests.